THREE-DIMENSIONAL DIFFUSION IN ARBITRARY DOMAIN USING GENERALIZED COORDINATES FOR THE BOUNDARY CONDITION OF THE FIRST KIND

Vera Solange de Oliveira Farias vera-solange@uol.com.br
Universidade Federal dos Vales do Jequitinhonha e Mucuri, Rodovia MG 367, Km 583, Nº 5.000, Diamantina/MG Brasil

Wilton Pereira da Silva wiltonps@uol.com.br
Cleide Maria Diniz Pereira da Silva e Silva cleidedps@uol.com.br
Pedro Luiz do Nascimento pedro@df.ufcg.edu.br
Antonio Gilson Barbosa de Lima gilson@dem.ufcg.edu.br
Universidade Federal de Campina Grande, Rua Aprígio Veloso, 882, Bodocongó, Campina Grande/PB Brasil

Abstract. *This work presents a three-dimensional numerical solution for the diffusion equation in transient state, in an arbitrary domain. To this end, the diffusion equation was discretized using the finite volume method with a fully implicit formulation and generalized coordinates, for the equilibrium boundary condition. For each time step, the system of equations obtained for a given structured mesh was solved by the Gauss-Seidel method. The computational code was developed in FORTRAN, using the CFV 6.6.0 studio, in a Windows Vista platform. The proposed solution was validated using analytical and numerical solutions of diffusion equation for two geometries. The geometries tested enabled to validate both orthogonal and non-orthogonal meshes. The analysis and comparison of the results showed that the proposed solution provides correct results for all cases investigated.*

Keywords*: generalized coordinates, arbitrary geometry, numerical simulation.*

1. INTRODUCTION

Diffusion is one of the transportation mechanisms in which the transfer of matter or energy occurs by molecular motion due to the existence of a concentration gradient of a substance or temperature, whereas the medium remains stationary. This process is represented by the diffusion equation, derived from the general equation of transport, which, depending on the problem may be called of Fick's Law or Fourier's Law.

Several physical phenomena use the diffusion theory with the aim of describing the transport of matter and energy in a medium. Most notably, we can mention the heating, cooling and freezing of products, as well as the drying process of porous materials. By looking at the literature, one can find several analytical and/or numerical solutions of the diffusion equation for various geometries and boundary conditions, treating the diffusion coefficients as constants or variables (Luikov; 1968; Crank, 1992; Lima, 1999; Silva et al., 2007; Hacihafizoğlu et al., 2008; Silva et. al., 2008; Silva, 2010; Silva et al., 2010).

The solution of the diffusion equation in various physical situations of interest, often requires the need to establish certain assumptions in describing the physical process. One of them is related to the geometry of the body in which occurs the transport of matter or energy. Several studies have been reported in literature using the diffusive model to describe the physical process, and consider the geometric shape of the bodies as cylinders, spheres or infinite slab (Silva, 2010; Chemkhi and Zagrouba, 2005; Saykova et al., 2009). For these simpler geometries, the diffusion equation can be solved analytically, and often constant thermophysical properties for the medium is assumed (Crank, 1992; Amendola and Queiroz, 2007; Saykova et al., 2009). These geometric simplifications also facilitate the numerical solution of the diffusion equation (Ukrainczyk, 2009). However, although this procedure usually presents good results, sometimes it does not adequately describe the processes involved, if the geometric shape of the solid under study is too different from the one considered.

One can also find in the literature, several applications of the diffusion model to bodies with other shapes, such as oblate and prolate spheroidal solids, (Lima 1999, Lima and Nebra, 2000, Li et al. 2004; Hacihafizoğlu et al. 2008; Melo et al. 2008; Carmo and Lima, 2008).

When it comes to solving the diffusion equation written in Cartesian coordinates for 3D geometries, one can cite Nascimento (2002), who presented various mathematical models to solve problems of transient diffusion, but for a specific geometry: solids in the shape of a parallelepiped. Other studies using Cartesian coordinates to solve the 3D diffusion equation can be found in the literature (Cadé et al., 2005, Nascimento et al., 2006; Saykova et al., 2009).

One can also find reported in the literature some studies that take into account the arbitrary geometry of bodies, and thus make use of generalized coordinates for solving numerically the diffusion equation by means of two-dimensional models. Among them, one can highlight the work of Salinas et al. (2004), Silva (2007); Silva et al. (2007);Silva et al. (2008); Silva et al. (2009); Silva et al (2010). Wu et al. (2004) proposed a three-dimensional numerical solution for an ellipsoid, and in this solution constant thermo-physical parameters were assumed, as well as an orthogonal structured grid.

Therefore, one can observe that there is abundant literature available on diffusion models in general. However, there is a lack of studies that take into account the arbitrary geometry of bodies though three-dimensional models, which is necessary in order to describe more precisely the process when the bodies under study show a complex geometric shape.

This paper proposes to model and present the numerical solution of three-dimensional diffusion equation written in generalized coordinates, using structured meshes and using the method of the finite volumes for a fully implicit formulation. The model should consider the arbitrary geometry of the bodies and provide a boundary condition of first kind. It should also consider constant, the transport parameters, as well as the dimensions of the solid. In order to numerically solve the diffusion equation, a computer code in Fortran language has been developed.

2. MATERIAL AND METHODS

2.1. Diffusion equation

The diffusion equation in Cartesian coordinates is given by (Bird, 2001; Maliska, 2004):

$$\frac{\partial(\lambda\Phi)}{\partial t}=\frac{\partial}{\partial x}\left(\Gamma^{\Phi}\frac{\partial\Phi}{\partial x}\right)+\frac{\partial}{\partial y}\left(\Gamma^{\Phi}\frac{\partial\Phi}{\partial y}\right)+\frac{\partial}{\partial z}\left(\Gamma^{\Phi}\frac{\partial\Phi}{\partial z}\right)+S \tag{1}$$

where t is the time, x, y and z are the Cartesian coordinates of position, λ and Γ^{Φ} are transport coefficients, S is a source term and Φ is the dependent variable to be determined. Equation (1) is frequently named diffusion equation of the physical domain, in contrast to the transformed domain.

In general, Cartesian coordinates are not appropriate to solve diffusion problems for solids of arbitrary shape. Thus, a coordinate system whose axes coincide with the borders of the control volumes of the studied solid will be used. This means that the new axes, denoted by ξ, η and γ, defining a curvilinear, non-orthogonal coordinates system must be used (Boas, 1983; Patankar, 1980; Maliska, 2004; Silva, 2007).

The curvilinear coordinates can be expressed as functions of x, y and z through mutual transformations of the type

$$\xi=\xi(x,y,z);\ \eta=\eta(x,y,z)\ \text{and}\ \gamma=\gamma(x,y,z). \tag{2}$$

Then, the diffusion equation can be written in the new coordinate system as (Maliska, 2004; Wu et al., 2004):

$$\frac{\partial}{\partial\tau}\left(\frac{\lambda\Phi}{J}\right)=\frac{\partial}{\partial\xi}\left[\left(\alpha_{11}\frac{\partial\Phi}{\partial\xi}+\alpha_{12}\frac{\partial\Phi}{\partial\eta}+\alpha_{13}\frac{\partial\Phi}{\partial\gamma}\right)J\Gamma^{\Phi}\right]+\frac{\partial}{\partial\eta}\left[\left(\alpha_{21}\frac{\partial\Phi}{\partial\xi}+\alpha_{22}\frac{\partial\Phi}{\partial\eta}+\alpha_{23}\frac{\partial\Phi}{\partial\gamma}\right)J\Gamma^{\Phi}\right]+$$
$$\frac{\partial}{\partial\gamma}\left[\left(\alpha_{31}\frac{\partial\Phi}{\partial\xi}+\alpha_{32}\frac{\partial\Phi}{\partial\eta}+\alpha_{33}\frac{\partial\Phi}{\partial\gamma}\right)J\Gamma^{\Phi}\right]+\frac{S}{J} \tag{3}$$

where τ is the time in transformed domain and the coefficients α_{ij} are given by expressions:

$$\alpha_{11}=\frac{1}{J^2}(\xi_x^2+\xi_y^2+\xi_z^2)\ ;\qquad \alpha_{12}=\alpha_{21}=\frac{1}{J^2}(\xi_x\eta_x+\xi_y\eta_y+\xi_z\eta_z)\ ;\qquad \alpha_{23}=\alpha_{32}=\frac{1}{J^2}(\eta_x\gamma_x+\eta_y\gamma_y+\eta_z\gamma_z);$$
$$\alpha_{22}=\frac{1}{J^2}(\eta_x^2+\eta_y^2+\eta_z^2)\ ;\qquad \alpha_{13}=\alpha_{31}=\frac{1}{J^2}(\xi_x\gamma_x+\xi_y\gamma_y+\xi_z\gamma_z)\qquad \alpha_{33}=\frac{1}{J^2}(\gamma_x^2+\gamma_y^2+\gamma_z^2)\ ; \tag{4a-f}$$

On the other hand, J is the Jacobian of the transformation and is defined by the determinant:

$$\frac{1}{J}\ =\ \det\begin{bmatrix}x_\xi & x_\eta & x_\gamma\\ y_\xi & y_\eta & y_\gamma\\ z_\xi & z_\eta & z_\gamma\end{bmatrix} \tag{5}$$

Equation (3) is often called the diffusion equation in the transformed domain.

2.2 Numerical Solution: discretization of the diffusion equation

The method used in the discretization of the diffusion equation is the finite volume method with a fully implicit formulation. The reason for this choice is that the solution becomes unconditionally stable for any time interval (Maliska, 2004).

Integrating Eq. (3) about space $\Delta\xi\,\Delta\eta\,\Delta\gamma$ and time ($\Delta\tau$) we obtain the following result:

$$\begin{aligned}\frac{\lambda_P\Phi_P-\lambda_P^0\Phi_P^0}{J_P}\frac{\Delta\xi\Delta\eta\Delta\gamma}{\Delta\tau} &= \alpha_{11e}J_e\,\Gamma_e^{\Phi}\Delta\eta\Delta\gamma\left.\frac{\partial\Phi}{\partial\xi}\right|_e + \alpha_{12e}J_e\Gamma_e^{\Phi}\Delta\eta\Delta\gamma\left.\frac{\partial\Phi}{\partial\eta}\right|_e + \alpha_{13e}J_e\,\Gamma_e^{\Phi}\Delta\eta\Delta\gamma\left.\frac{\partial\Phi}{\partial\gamma}\right|_e - \\ \alpha_{11w}J_w\,\Gamma_w^{\Phi}\Delta\eta\Delta\gamma\left.\frac{\partial\Phi}{\partial\xi}\right|_w &- \alpha_{12w}J_w\Gamma_w^{\Phi}\Delta\eta\Delta\gamma\left.\frac{\partial\Phi}{\partial\eta}\right|_w - \alpha_{13w}J_w\,\Gamma_w^{\Phi}\Delta\eta\Delta\gamma\left.\frac{\partial\Phi}{\partial\gamma}\right|_w + \alpha_{21n}J_n\,\Gamma_n^{\Phi}\Delta\xi\Delta\gamma\left.\frac{\partial\Phi}{\partial\xi}\right|_n + \\ \alpha_{22n}J_n\Gamma_n^{\Phi}\Delta\xi\Delta\gamma\left.\frac{\partial\Phi}{\partial\eta}\right|_n &+ \alpha_{23n}J_n\,\Gamma_n^{\Phi}\Delta\xi\Delta\gamma\left.\frac{\partial\Phi}{\partial\gamma}\right|_n - \alpha_{21s}J_s\,\Gamma_s^{\Phi}\Delta\xi\Delta\gamma\left.\frac{\partial\Phi}{\partial\xi}\right|_s - \alpha_{22s}J_s\Gamma_s^{\Phi}\Delta\xi\Delta\gamma\left.\frac{\partial\Phi}{\partial\eta}\right|_s - \\ \alpha_{23s}J_S\,\Gamma_S^{\Phi}\Delta\xi\Delta\eta\left.\frac{\partial\Phi}{\partial\gamma}\right|_s &+ \alpha_{31f}J_f\,\Gamma_f^{\Phi}\Delta\xi\Delta\eta\left.\frac{\partial\Phi}{\partial\xi}\right|_f + \alpha_{32f}J_f\Gamma_f^{\Phi}\Delta\xi\Delta\eta\left.\frac{\partial\Phi}{\partial\eta}\right|_f + \alpha_{33f}J_f\,\Gamma_f^{\Phi}\Delta\xi\Delta\eta\left.\frac{\partial\Phi}{\partial\gamma}\right|_f \\ - \alpha_{31b}J_b\,\Gamma_b^{\Phi}\Delta\xi\Delta\eta\left.\frac{\partial\Phi}{\partial\xi}\right|_b &- \alpha_{32b}J_b\Gamma_b^{\Phi}\Delta\xi\Delta\eta\left.\frac{\partial\Phi}{\partial\eta}\right|_b - \alpha_{33b}J_b\,\Gamma_b^{\Phi}\Delta\xi\Delta\eta\left.\frac{\partial\Phi}{\partial\gamma}\right|_b + \frac{S_P\Phi_P}{J_P}\Delta\xi\Delta\eta\Delta\gamma + \frac{S_C}{J_P}\Delta\xi\Delta\eta\Delta\gamma\end{aligned} \tag{6}$$

where the superscript 0 means "former time" and its absence means "current time". The subscripts *"e", "w", "n", "s"*, "f" and "b" mean the east, west, north, south, front and back borders, respectively, of an elementary generating cell of a control volume, while *P* is the nodal point of this volume. All the elements described above are shown in Fig. 1.

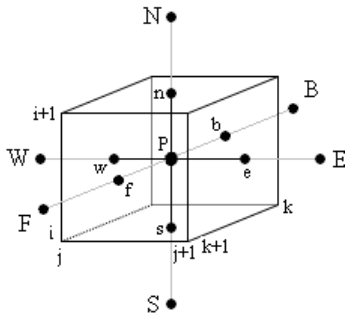

Figure 1: Control volume with a nodal point P and the faces "e", "w", "n", "s", "f" e "b".

In order to complete the discretization of Eq. (6), it should be noted that for a three-dimensional non-orthogonal structured mesh created to represent a solid with any geometry, there are 27 different types of control volumes in the transformed domain, as shown in Fig. 2. Obviously, each control volume shown in Fig. 2 generates an algebraic equation distinct from the discretization of Eq. (6).

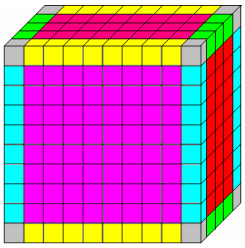

Figure 2: Regions with 27 different types of control volumes in the transformed domain for a three- dimensional structured mesh.

The discretization of Eq. (6) for the internal control volumes (Fig. 1) results in the following equations for the direct derivatives of the variable Φ:

$$\left.\frac{\partial\Phi}{\partial\xi}\right|_e = \frac{\Phi_E - \Phi_P}{\Delta\xi}; \quad \left.\frac{\partial\Phi}{\partial\xi}\right|_w = \frac{\Phi_P - \Phi_W}{\Delta\xi}; \quad \left.\frac{\partial\Phi}{\partial\eta}\right|_n = \frac{\Phi_N - \Phi_P}{\Delta\eta};$$

$$\left.\frac{\partial\Phi}{\partial\eta}\right|_s = \frac{\Phi_P - \Phi_S}{\Delta\eta}; \quad \left.\frac{\partial\Phi}{\partial\gamma}\right|_f = \frac{\Phi_F - \Phi_P}{\Delta\gamma}; \quad \left.\frac{\partial\Phi}{\partial\gamma}\right|_b = \frac{\Phi_P - \Phi_B}{\Delta\gamma}. \tag{7a-f}$$

The expressions for the cross derivatives are defined as follows:

$$\left.\frac{\partial\Phi}{\partial\eta}\right|_e = \frac{\Phi_N + \Phi_{NE} - \Phi_S - \Phi_{SE}}{4\Delta\eta}; \quad \left.\frac{\partial\Phi}{\partial\eta}\right|_w = \frac{\Phi_N + \Phi_{NW} - \Phi_S - \Phi_{SW}}{4\Delta\eta}; \quad \left.\frac{\partial\Phi}{\partial\eta}\right|_f = \frac{\Phi_N + \Phi_{FN} - \Phi_S - \Phi_{FS}}{4\Delta\eta}$$

$$\left.\frac{\partial\Phi}{\partial\eta}\right|_b = \frac{\Phi_N + \Phi_{BN} - \Phi_S - \Phi_{BS}}{4\Delta\eta}; \quad \left.\frac{\partial\Phi}{\partial\xi}\right|_n = \frac{\Phi_E + \Phi_{NE} - \Phi_W - \Phi_{NW}}{4\Delta\xi}; \quad \left.\frac{\partial\Phi}{\partial\xi}\right|_s = \frac{\Phi_E + \Phi_{SE} - \Phi_W - \Phi_{SW}}{4\Delta\xi};$$

$$\left.\frac{\partial\Phi}{\partial\xi}\right|_f = \frac{\Phi_E + \Phi_{FE} - \Phi_W - \Phi_{FW}}{4\Delta\xi}; \quad \left.\frac{\partial\Phi}{\partial\xi}\right|_b = \frac{\Phi_E + \Phi_{BE} - \Phi_W - \Phi_{BW}}{4\Delta\xi}; \quad \left.\frac{\partial\Phi}{\partial\gamma}\right|_e = \frac{\Phi_F + \Phi_{FE} - \Phi_B - \Phi_{BE}}{4\Delta\gamma};$$

$$\left.\frac{\partial\Phi}{\partial\gamma}\right|_w = \frac{\Phi_F + \Phi_{FW} - \Phi_B - \Phi_{BW}}{4\Delta\gamma}; \quad \left.\frac{\partial\Phi}{\partial\gamma}\right|_n = \frac{\Phi_F + \Phi_{FN} - \Phi_B - \Phi_{BN}}{4\Delta\gamma}; \quad \left.\frac{\partial\Phi}{\partial\gamma}\right|_s = \frac{\Phi_F + \Phi_{FS} - \Phi_B - \Phi_{BS}}{4\Delta\gamma}. \tag{8a-l}$$

The resulting algebraic equation for the volumes of internal control is given by:

$$A_p\Phi_P = A_e\Phi_E + A_w\Phi_W + A_n\Phi_N + A_s\Phi_S + A_f\Phi_F + A_b\Phi_B + A_{ne}\Phi_{NE} + A_{nw}\Phi_{NW} + A_{se}\Phi_{SE} + A_{sw}\Phi_{SW} +$$
$$A_{fe}\Phi_{FE} + A_{fw}\Phi_{FW} + A_{be}\Phi_{BE} + A_{bw}\Phi_{BW} + A_{fn}\Phi_{FN} + A_{fs}\Phi_{FS} + A_{bn}\Phi_{BN} + A_{bs}\Phi_{BS} + B \tag{9}$$

where some coefficients are given by:

$$A_P = \frac{\lambda_P}{J_P}\frac{\Delta\xi\Delta\eta\Delta\gamma}{\Delta\tau} + \frac{\Delta\eta\Delta\gamma}{\Delta\xi}\alpha_{11e}J_e\Gamma_e^\Phi + \frac{\Delta\eta\Delta\gamma}{\Delta\xi}\alpha_{11w}J_w\Gamma_w^\Phi + \frac{\Delta\xi\Delta\gamma}{\Delta\eta}\alpha_{22n}J_n\Gamma_n^\Phi + \frac{\Delta\xi\Delta\gamma}{\Delta\eta}\alpha_{22s}J_s\Gamma_s^\Phi +$$
$$\frac{\Delta\xi\Delta\eta}{\Delta\gamma}\alpha_{33f}J_f\Gamma_f^\Phi + \frac{\Delta\xi\Delta\eta}{\Delta\gamma}\alpha_{33b}J_b\Gamma_b^\Phi - \frac{S_P}{J_P}\Delta\xi\Delta\eta\Delta\gamma;$$

$$A_e = \frac{\Delta\eta\Delta\gamma}{\Delta\xi}\alpha_{11e}J_e\Gamma_e^\Phi + \frac{\Delta\gamma}{4}\alpha_{21n}J_n\Gamma_n^\Phi - \frac{\Delta\gamma}{4}\alpha_{21s}J_s\Gamma_s^\Phi + \frac{\Delta\eta}{4}\alpha_{31f}J_f\Gamma_f^\Phi - \frac{\Delta\eta}{4}\alpha_{31b}J_b\Gamma_b^\Phi;$$

.....

$$A_n = \frac{\Delta\xi\Delta\gamma}{\Delta\eta}\alpha_{22n}J_n\Gamma_n^\Phi + \frac{\Delta\gamma}{4}\alpha_{12e}J_e\Gamma_e^\Phi - \frac{\Delta\gamma}{4}\alpha_{12w}J_w\Gamma_w^\Phi + \frac{\Delta\xi}{4}\alpha_{32f}J_f\Gamma_f^\Phi - \frac{\Delta\xi}{4}\alpha_{32b}J_b\Gamma_b^\Phi;$$

..... (10a-k)

$$A_f = \frac{\Delta\xi\Delta\eta}{\Delta\gamma}\alpha_{33f}J_f\Gamma_f^\Phi + \frac{\Delta\eta}{4}\alpha_{13e}J_e\Gamma_e^\Phi - \frac{\Delta\eta}{4}\alpha_{13w}J_w\Gamma_w^\Phi + \frac{\Delta\xi}{4}\alpha_{23n}J_n\Gamma_n^\Phi - \frac{\Delta\xi}{4}\alpha_{23s}J_s\Gamma_s^\Phi;$$

.....

$$A_{ne} = \frac{\Delta\gamma}{4}\alpha_{12e}J_e\Gamma_e^\Phi + \frac{\Delta\gamma}{4}\alpha_{21n}J_n\Gamma_n^\Phi; \quad A_{se} = -\frac{\Delta\gamma}{4}\alpha_{12e}J_e\Gamma_e^\Phi - \frac{\Delta\gamma}{4}\alpha_{21s}J_s\Gamma_s^\Phi;$$

.....

$$A_{fe} = \frac{\Delta\eta}{4}\alpha_{13e}J_e\Gamma_e^\Phi + \frac{\Delta\eta}{4}\alpha_{31f}J_f\Gamma_f^\Phi; \quad A_{be} = -\frac{\Delta\eta}{4}\alpha_{13e}J_e\Gamma_e^\Phi - \frac{\Delta\eta}{4}\alpha_{31b}J_b\Gamma_b^\Phi;$$

.....

$$A_{fn} = \frac{\Delta\xi}{4}\ \alpha_{23n} J_n\ \Gamma_n^{\Phi} + \frac{\Delta\xi}{4}\alpha_{32f} J_f\ \Gamma_f^{\Phi}; \qquad A_{bn} = -\frac{\Delta\xi}{4}\ \alpha_{23n} J_n\ \Gamma_n^{\Phi} - \frac{\Delta\xi}{4}\alpha_{32b} J_b\ \Gamma_b^{\Phi};$$

$$B = \frac{\lambda_P^0 \Phi_P^0}{J_P}\frac{\Delta\xi\Delta\eta\Delta\gamma}{\Delta\tau} + \frac{S_C}{J_P}\Delta\xi\Delta\eta\Delta\gamma$$

Often, the lines ξ, η and γ of a mesh in the transformed domain are identified by consecutive integers, and thus $\Delta\xi$, $\Delta\eta$ and $\Delta\gamma$ are equal to unity in all equations as they appear.

3.2 Metrics on nodal points and faces of control volumes

The determination of the terms α_{ij} and the Jacobian J requires the knowledge of the metrics of the transformation, since they are calculated from the inverse metric, which in turn should be determined by the partial derived x_ξ, x_η, x_γ, y_ξ, y_η, y_γ, z_ξ, z_η and z_γ. That way, should be established expressions for these derived for both the nodal point P as for all the faces of control volumes. Thus, for a nodal point P of an internal control volume of a mesh, the direct derivative of the coordinates x with respect to ξ, η and γ are given by the following expressions:

$$x_\xi^P = \frac{x_e - x_w}{\Delta\xi}; \qquad x_\eta^P = \frac{x_n - x_s}{\Delta\eta}; \qquad x_\gamma^P = \frac{x_f - x_b}{\Delta\gamma} \tag{11a - c}$$

where x_e, x_w, x_n, x_s, x_f and x_b are the coordinates of the midpoints of the faces "e", "w", "n", "s", "f" e "b", respectively, and are calculated as the arithmetic mean of the four vertices that form the quadrilateral face. The derivatives related to the coordinates *y* and *z* are obtained following the same steps above.

On the borders of each control volume, for example, "e" (between control volumes P and E), the following expression should be used to determine the derivatives of the coordinates *x* with respect to ξ, η and γ:

$$x_\xi^e = \frac{x_E - x_P}{\Delta\xi} = \frac{1}{2\Delta\xi}\left[\frac{x_{i,j+2,k} + x_{i+1,j+2,k} + x_{i+1,j+2,k+1} + x_{i,j+2,k+1}}{4} - \frac{x_{i,j,k+1} + x_{i+1,j,k+1} + x_{i+1,j,k} + x_{i,j,k}}{4}\right]$$

$$x_\eta^e = \frac{1}{\Delta\eta}\left[\frac{x_{i+1,j+1,k+1} + x_{i+1,j+1,k}}{2} - \frac{x_{i,j+1,k+1} + x_{i,j+1,k}}{2}\right]; \quad x_\gamma^e = \frac{1}{\Delta\gamma}\left[\frac{x_{i,j+1,k+1} + x_{i+1,j+1,k+1}}{2} - \frac{x_{i+1,j+1,k} + x_{i,j+1,k}}{2}\right] \tag{12a-c}$$

where x_P and x_E are the coordinates of the nodal point P and its east side borderer (E), which can be calculated by the arithmetic average of the eight vertices of the parallelepiped representing the volume control. Similar expressions can be found for the derivatives related to the other coordinates. In a similar analysis, we obtain the derivatives on the other sides as well as the coordinates of nodal points located in the neighboring control volumes.

With a similar procedure as that presented above for the internal control volumes of a mesh, algebraic equations can also be determined for each control volume located in the boundaries of the mesh defined by the solid in study. As example, for the convective boundary condition, the discretization of the diffusion equation will be presented for a control volume located in the west boundary, shown in the fragment of mesh in the transformed domain, in Fig. 3. It can be observed that this control volume has no neighbor on the west side.

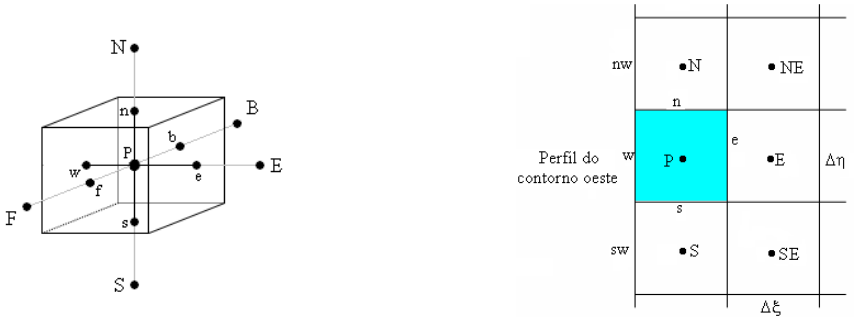

Figure 3: (a) Control volume P located on the west side border of the transformed domain; (b) side view of the west border.

The derivatives that differ from those determined for the internal control volumes are dependent on the western boundary and can be written as:

$$\left.\frac{\partial \Phi}{\partial \xi}\right|_w = \frac{\Phi_P - \Phi_w}{\frac{\Delta\xi}{2}}; \qquad \left.\frac{\partial \Phi}{\partial \eta}\right|_w = \frac{\Phi_{nw} - \Phi_{sw}}{2\Delta\eta}; \qquad \left.\frac{\partial \Phi}{\partial \gamma}\right|_w = \frac{\Phi_{fw} - \Phi_{bw}}{2\Delta\gamma}; \tag{13a-g}$$

$$\left.\frac{\partial \Phi}{\partial \xi}\right|_n = \frac{1}{\Delta\xi}\left[\frac{\Phi_P + \Phi_N + \Phi_E + \Phi_{NE}}{4} - \frac{\left(\Phi_w + \Phi_{nw}\right)}{2}\right]; \qquad \left.\frac{\partial \Phi}{\partial \xi}\right|_s = \frac{1}{\Delta\xi}\left[\frac{\Phi_P + \Phi_S + \Phi_E + \Phi_{SE}}{4} - \frac{\left(\Phi_w + \Phi_{sw}\right)}{2}\right];$$

$$\left.\frac{\partial \Phi}{\partial \xi}\right|_f = \frac{1}{\Delta\xi}\left[\frac{\Phi_P + \Phi_F + \Phi_E + \Phi_{FE}}{4} - \frac{\left(\Phi_w + \Phi_{fw}\right)}{2}\right]; \qquad \left.\frac{\partial \Phi}{\partial \xi}\right|_b = \frac{1}{\Delta\xi}\left[\frac{\Phi_P + \Phi_B + \Phi_E + \Phi_{BE}}{4} - \frac{\left(\Phi_w + \Phi_{bw}\right)}{2}\right];$$

Replacing the derivatives mentioned in equation above in Eq. (6), one can find the following algebraic equation for the control volumes located on the west side of the inner grip:

$$A_p\Phi_P = A_e\Phi_E + A_n\Phi_N + A_s\Phi_S + A_f\Phi_F + A_b\Phi_B + A_{ne}\Phi_{NE} + A_{se}\Phi_{SE} + A_{fe}\Phi_{FE} + A_{be}\Phi_{BE} + A_{fn}\Phi_{FN} + A_{fs}\Phi_{FS} + A_{bn}\Phi_{BN} + A_{bs}\Phi_{BS} + B \tag{14}$$

Some of the terms that differ from those determined for the internal volumes are given by:

$$A_P = \frac{\lambda_P}{J_P}\frac{\Delta\xi\Delta\eta\Delta\gamma}{\Delta\tau} + \frac{\Delta\eta\Delta\gamma}{\Delta\xi}\,\alpha_{11e}J_e\,\Gamma_e^{\Phi} + \frac{\Delta\eta\Delta\gamma}{\Delta\xi}2\,\alpha_{11w}J_w\,\Gamma_w^{\Phi} + \frac{\Delta\xi\Delta\gamma}{\Delta\eta}\,\alpha_{22n}J_n\,\Gamma_n^{\Phi} + \frac{\Delta\xi\Delta\gamma}{\Delta\eta}\,\alpha_{22s}J_s\,\Gamma_s^{\Phi} +$$
$$\frac{\Delta\xi\Delta\eta}{\Delta\gamma}\,\alpha_{33f}J_f\,\Gamma_f^{\Phi} + \frac{\Delta\xi\Delta\eta}{\Delta\gamma}\,\alpha_{33b}J_b\,\Gamma_b^{\Phi} - \frac{S_P}{J_P}\Delta\xi\Delta\eta\Delta\gamma - \frac{\Delta\gamma}{4}\alpha_{21n}J_n\,\Gamma_n^{\Phi} + \frac{\Delta\gamma}{4}\alpha_{21s}J_s\,\Gamma_s^{\Phi} - \frac{\Delta\eta}{4}\alpha_{31f}J_f\,\Gamma_f^{\Phi} +$$
$$\frac{\Delta\eta}{4}\alpha_{31b}J_b\,\Gamma_b^{\Phi};$$

$$A_n = \frac{\Delta\xi\Delta\gamma}{\Delta\eta}\,\alpha_{22n}J_n\,\Gamma_n^{\Phi} + \frac{\Delta\gamma}{4}\,\alpha_{12e}J_e\,\Gamma_e^{\Phi} + \frac{\Delta\gamma}{4}\,\alpha_{21n}J_n\,\Gamma_n^{\Phi} + \frac{\Delta\xi}{4}\alpha_{32f}J_f\,\Gamma_f^{\Phi} - \frac{\Delta\xi}{4}\alpha_{32b}J_b\,\Gamma_b^{\Phi};$$

(15a-e)

$$A_{bn} = -\frac{\Delta\xi}{4}\,\alpha_{23n}J_n\,\Gamma_n^{\Phi} - \frac{\Delta\xi}{4}\alpha_{32b}J_b\,\Gamma_b^{\Phi}; \qquad A_{bs} = \frac{\Delta\xi}{4}\,\alpha_{23s}J_s\,\Gamma_s^{\Phi} + \frac{\Delta\xi}{4}\alpha_{32b}J_b\,\Gamma_b^{\Phi};$$

$$B = \frac{\lambda_P^0\Phi_P^0}{J_P}\frac{\Delta\xi\Delta\eta\Delta\gamma}{\Delta\tau} + \frac{S_C}{J_P}\Delta\xi\Delta\eta\Delta\gamma + \frac{\Delta\eta\Delta\gamma}{\Delta\xi}2\,\alpha_{11w}J_w\,\Gamma_w^{\Phi}\Phi_w - \frac{\Delta\gamma}{2}\alpha_{12w}J_w\,\Gamma_w^{\Phi}\left(\Phi_{nw} - \Phi_{sw} - \frac{\Delta\eta}{2}\alpha_{13w}J_w\,\Gamma_w^{\Phi}\left(\Phi_{fw} - \Phi_{sw}\right)\right)$$
$$-\frac{\Delta\gamma}{2}\alpha_{21n}J_n\,\Gamma_n^{\Phi}\left(\Phi_w + \Phi_{nw}\right) + \frac{\Delta\gamma}{2}\alpha_{21s}J_s\,\Gamma_s^{\Phi}\left(\Phi_w + \Phi_{sw}\right) - \frac{\Delta\eta}{2}\alpha_{31f}J_f\,\Gamma_f^{\Phi}\left(\Phi_w + \Phi_{fw}\right) + \frac{\Delta\eta}{2}\alpha_{31b}J_b\,\Gamma_b^{\Phi}\left(\Phi_w + \Phi_{bw}\right)$$

With a procedure similar to that presented to the internal control volumes, one can also determine the metrics for the control volume located on the inner face of the western border and algebraic equations similar to the above can be found for each control volume located on the boundary of the solid.

Once determined the values of Φ for each control volume, an instant t, the average value of the variable at this moment can be determined by the expression given below, with appropriate discretization:

$$\overline{\Phi}(t) = \frac{\int_V \Phi(x,y,z,t)dV}{\int_V dV}; \qquad \overline{\Phi} = \frac{1}{\sum\frac{1}{J_P}}\sum\Phi_P\,\frac{1}{J_P} \tag{16a-b}$$

The computer code proposed in this paper was developed in the Windows Vista platform through the use of the Compaq Visual Fortran studio, version 6.6.0 Professional Edition, using the programming QuickWin Application, and for its validation, simulations were performed for which a numerical or analytical solution is known.

3 RESULTS AND DISCUSSION

Many tests were performed in order to validate the proposed numerical model and results are available in Farias (2010). In this paper we present a simulation aimed at validating the proposed code using analytical solutions (parallelepiped) and a simulation to validate the code through numerical solutions.

3.1 Validation of the numerical solution proposed through analytical solutions

In this test, we assumed a constant and equal value to the unit for λ, a uniform initial distribution to Φ (Φ_i = 0.2381) was assumed and the transport coefficients as well as the dimensions of the solid were considered constant. Moreover, the same magnitude equilibrium value was assumed on all sides of the solid (Φ_{eq} = 0.0133) and simulated for the effective diffusivity, the value of Γ^{Φ} = 6.93931 x10^{-10} m^2 s^{-1}

The scheme simulating a parallelepiped with dimensions L_1 = 6.02 x10^{-3} m, L_2 = 46.16 x10^{-3} m and L_3 = 86.74x10^{-3} m, is shown in Figure 4.

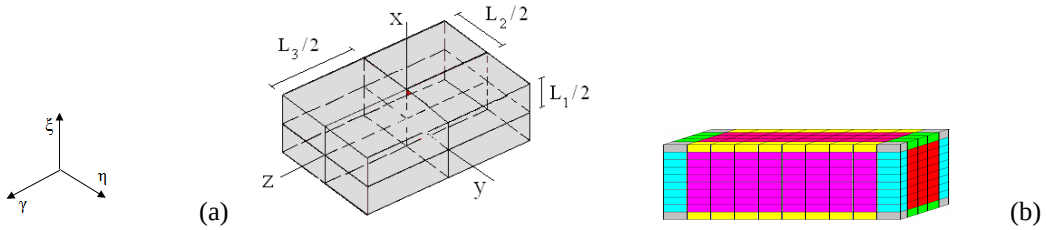

Figure 4: Parallelepiped (not on scale) used to validate the numerical solution proposed for the three-dimensional diffusion equation via analytical solution (a) physical domain (b) computational domain.

In the numerical solution, the domain transformed involved a mesh with 18 ξ lines, 22 η lines, 26 γ lines and 2000 time steps for a range of Δt = 0.2725 min. The results from the analytical solution were obtained with the "Prescribed Adsorption-Desorption" software (http://zeus.df.ufcg.edu.br/labfit/Prescribed.htm). Using the LAB Fit Curve Fitting Software V 7.2.46, available at www.labfit.net, the graphs of the obtained solutions were generated in the same system of axes and are shown in Figure 5.

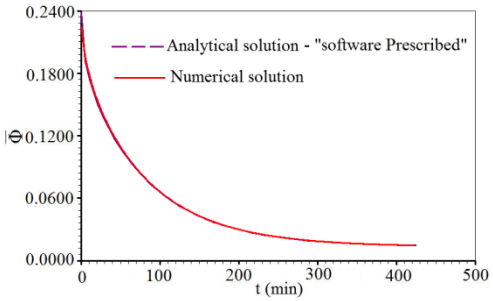

Figure 5: Superposition of the solutions obtained via the proposed numerical method and analytical method to the average value of the magnitude in a parallelepiped with prescribed boundary condition.

Through an observation of Figure 5, becomes visible that there is good conformity between the results obtained by both methods, since no distinction is observed between the curves. Therefore, it is possible to point out that the developed computer code is valid to calculate the average value of the magnitude.

3.2 Validation of the numerical solution proposed through numerical solutions

In order to validate the numerical solution proposed through numerical solutions, the simulation carried out involved consistency tests exploring symmetry conditions, temporal evolution of the spatial distribution and analysis of transient regimen of the magnitude in an arbitrarily chosen control volume.

The geometric figure used for the study of non-orthogonal meshes was of a solid obtained from extrusion along the *z* axis, a diamond in the *xy* plane, with the largest diagonal measuring twice the smallest diagonal. Figure 6 illustrates the

geometric situation treated highlighting the two-dimensional mesh which originated the solid, as well as the axes of the generalized coordinates and the Cartesian coordinates.

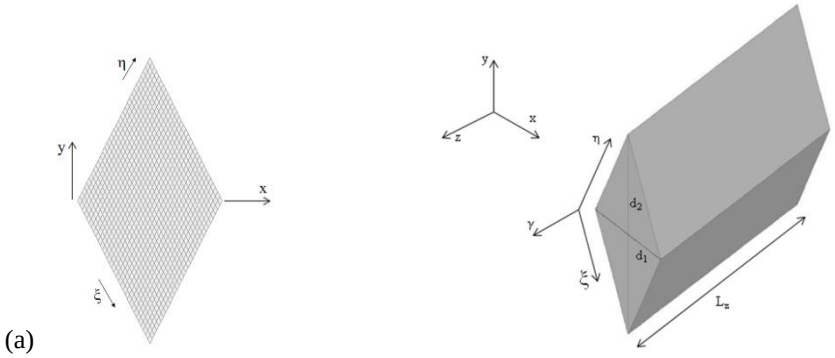

(a) (b)

Figure 6: Solid (not on scale) used in the validation of computational code proposed for non-orthogonal meshs (a) two-dimensional mesh that generated the solid; (b) solid generated by the extrusion of a diamond.

The physical parameters and the initial and shape conditions are summarized in Table 1.

Table 1: Physical parameters used to solve the diffusion equation in a non-orthogonal mesh for the prescribed boundary condition:

Φ_i	Φ_{eq}	Γ^{Φ} ($m^2 s^{-1}$)	d_1 (m)	d_2 (m)	L_z (m)
1.00	0.10	1.66667×10^{-7}	8.00×10^{-3}	16.00×10^{-3}	100.00×10^{-3}

The transformed domain involved a time interval Δt = 0.20 min. for 1000 time steps and a discretized mesh with 33 ξ lines, 33 η lines and 34 γ lines. In consistency tests for non-orthogonal structured meshs, we analyzed the transient of the knots corresponding to the control volume located on the opposite corners of the larger diagonal of the solid`s central surface and the superposition of solutions obtained for the two control volumes are shown in Figure 7a. Obtaining information about how the moisture level content differs inside and outside of the solid is important because these differences generate tensions that can damage the product. Therefore, we analyzed the transients to a boundary volume located in one of the corners of the larger diagonal, another one in one of the corners of the smaller diagonal and a lower internal control volume. The results are shown in Figure 7b.

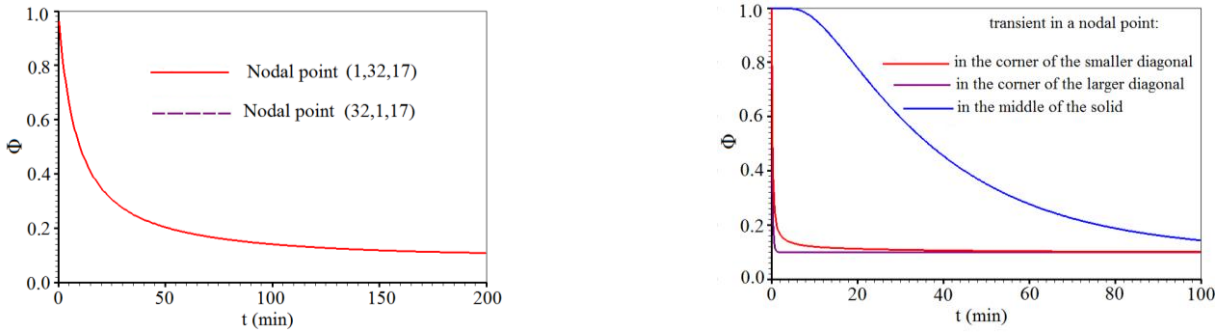

(a) (b)

Figure 7 - (a) Superposition of Φ transients, in a diamond, in the nodal points related to the control volumes located on the corners of the larger diagonal of the solid`s central surface.
(b) Results of Φ transient, obtained with the code proposed for a nodal point located in the middle of the solid, another one in the corner of the smaller diagonal, and one more in the corner of the larger diagonal.

Through an inspection of the results presented in Figure 7, it is possible to say that there is consistency in the results obtained by the proposed numerical solution for the physical phenomenon of the diffusion process expected for the non-orthogonal mesh studied. It can be observed that the diffusion occurs faster in the corners of the larger diagonal, being slower in the corners of the smaller diagonal and even slower in the control volumes located in the middle of the solid. It is also evident that the control volumes located on the edge almost instantly assume the equilibrium value, which is consistent with the imposition established by the boundary condition of first kind.

The Contour Plots software (http://zeus.df.ufcg.edu.br/labfit/Contour.zip) enables the visual analysis of the temporal evolution of spatial distribution of the Φ magnitude on a two-dimensional mesh in the physical domain. This option was used for the central surface of the solid with the results from the numerical code proposed in this paper. The time evolution was followed in several moments and the contour diagrams obtained are shown in Figure 8.

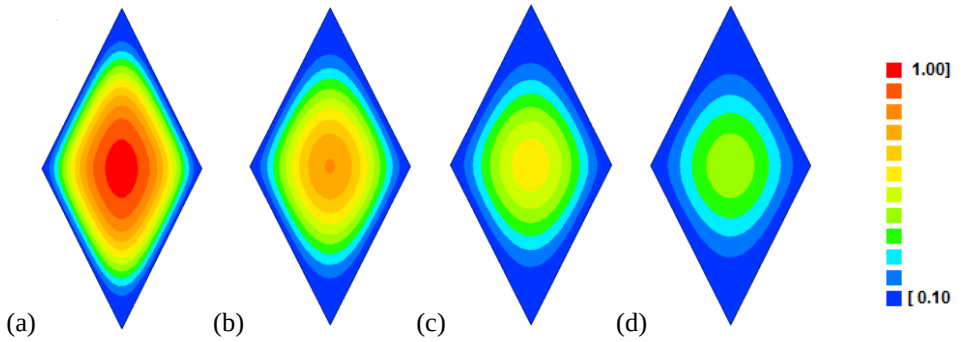

Figure 8: Contour plots for the central surface of the solid shown in Figure 6 for the moments:
a) t = 10 min, b) t = 20 min, c) t = 30 min, d) t = 40 min.

By observing the contour plots shown in Figure 8, it is clear that there is consistency in results, due to the fact that the edge assumes the equilibrium value almost instantly, a situation imposed by the balance boundary condition. In addition to that, the transportation occurs quite fast on the boundary, gradually diminishing as it moves inwards, until it becomes slow in the center of the solid. Therefore, it is clear that the proposed solution is consistent, since the symmetry condition exploited was consistent in all situations analyzed.

The computational code developed was validated through a comparison with the transients produced by the Diffusion RE software. Figure 9a shows the results for a control volume located inside the solid, identified by (ξ = 16, η = 16, γ = 17). Figure 9b illustrates the temporal evolution of the diffusion process to the average magnitude value, considering the volume control located in the central surface of the solid.

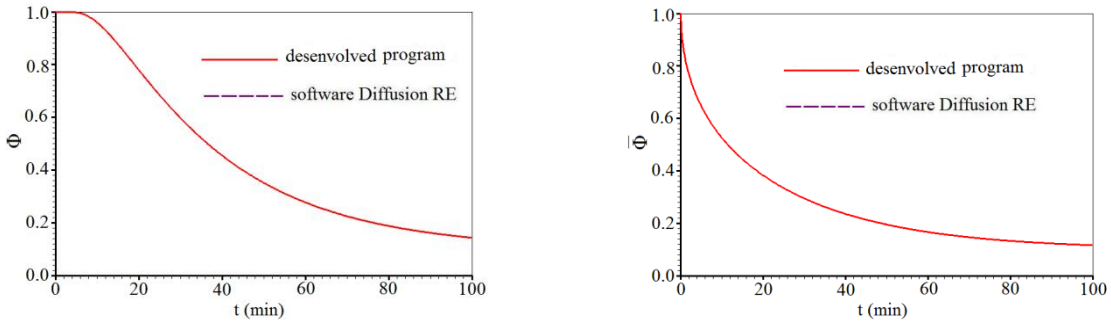

Figure 9: (a) Φ Transient (a) for a nodal point inside the solid, identified by (ξ = 16, η = 16, γ = 17)
(b) Transient for the average value of Φ in the central surface of the solid

4 CONCLUSION

The theory proposed in this paper for the numerical solution of the diffusion equation applied to solids with three-dimensional arbitrary geometries using generalized coordinates and making use of equilibrium boundary condition, produced results which were consistent with those expected. The comparison of the proposed numerical solution with the analytical solution of the diffusion equation for the parallelepiped also showed a consistent result, since there was a good conformity between the curves obtained from both solutions. Moreover, in all consistency tests that were performed by exploiting symmetry conditions, the results were satisfactory.

As for the validation of the computer code developed using numerical solutions, the results were consistent for the analyzed geometry (solid obtained from the extrusion of a diamond). When a comparison of the proposed solution was made with numerical solutions of the diffusion equation obtained with software available in the literature, the solutions obtained by both methods coincided in all analyzed situations.

It can be stated, therefore, that the computer code developed in this work is valid for a boundary condition of first kind and can be applied to the study of 3D diffusion phenomenon in solids with any geometry. Some examples of possible applications can be brought up, such as the mass transfer, heat conduction, drying of porous solids and cooling and freezing of bodies.

5. REFERENCES

Amendola, M.; Queiroz, M.R., 2007, Mathematical methodologies for calculating the mass diffusion coefficient of bananas during drying. Revista Brasileira de Engenharia Agrícola e Ambiental, v. 11, n. 6, p. 623-627.

Bird, R.B.; Stewart, W.E.; Lightfoot, E.N., Transport phenomena. 2nd Ed. New York: John Wiley & Sons, Inc., 2001, 912 p.

Boas, M.L., 1983, Mathematical methods in the physical sciences. New York: John Wiley & Sons, Inc., 783 p.

Cadê, M.A.; 2005, Nascimento, J.J.S.; Lima, A.G.B., Secagem de tijolos cerâmicos vazados: uma aproximação por volumes finitos. Revista Matéria, v. 10, n. 3, p. 433-453.

Carmo, J.E.F.; Lima, A.G.B., 2008, Mass transfer inside oblate spheroidal solids: modelling and simulation. Brazilian Journal of Chemical Engineering, v. 25, n. 1, p. 19-26.

Chemkhi, S.; Zagrouba, F. 2005, Water diffusion coefficient in clay material from drying data. Desalination, v.185, p 491-498.

Crank, J., 1992, The mathematics of diffusion, Oxford Science Publications, New York, 414 p.

Farias, V.S.O., 2010, Exame de Qualificação para a tese de Doutorado em Engenharia de Processos, Centro de Ciências e Tecnologia, Universidade Federal de Campina Grande, PB, Brasil

Hacihafizoğlu, O.; Cihan,A.; Kahveci, K.; Lima, A.G.B., 2008, A liquid diffusion model for thin-layer drying of rough rice. European Food Research and Technology, 226(4), doi: 10.1007/s00217-007-0593-0,.

Li, Z.; Kobayashi, N.; Hasatani, M., 2004 Modeling of diffusion in ellipsoidal solids: a comparative study. Drying Technology, v. 22, n. 4, p. 649-675.

Lima, A.G.B., 1999, Fenômeno de difusão em sólidos esferoidais prolatos. Estudo de caso: secagem de bananas, 244 p. Tese (Doutorado em Engenharia Mecânica), UNICAMP, São Paulo.

Lima, A.G.B.; Nebra, S.A., 2000, Theoretical analysis of the diffusion process inside prolate spheroidal solids. Drying Technology, 18 (1 - 2), p. 21-48.

Luikov, A.V., 1968, Analytical heat diffusion theory. Academic Press, New York and London, 684 p.

Maliska, C.R., 2004, Transferência de calor e mecânica dos fluidos computacional. LTC Editora S.A., R. Janeiro, 453 p.

Melo, J.C.S.; Lima, W.C.P.B.; Farias Neto, S.R.; Lima, A.G.B., 2008, Resfriamento de frutas com forma esferoidal prolata via método integral baseado em Galerkin. V Congresso Nacional de Engenharia Mecânica, Salvador, Bahia.

Nascimento, J.J.S., 2002, Fenômenos de difusão transiente em sólidos paralelepípedos. Estudo de caso: secagem de materiais cerâmicos, 181 p. Tese de Doutorado em Engenharia Mecânica, Centro de Tecnologia, UFPB.

Nascimento, J.J.S.; Lima, A.G.B.; Teruel, B.J.; Belo, F.A., 2006, Heat and mass transfer with schrinkage during the drying of ceramic bricks. Informacion Technologica, v. 17, n. 6, p. 145-151.

Patankar, S.V., 1980, Numerical heat tranfer and fluid flow. New York: Hemisphere Publishing Coorporation, 197 p.

Salinas, C.; Ananias, A.; Alvear, M., 2004, Simulación del secado de la madera: word drying simulation. Maderas, Ciência e Tecnologia, v. 6, n. 1, p. 3-18.

Saykova, I.; Cwicklinski, G.; Castelle, P., 2009, Analytical approach for predicting effective diffusion coefficients in multidimensional slab geometry. Journal of the University of Chemical Technology and Metallurgy, v. 44, 1, p. 44-49.

Silva, C.M.D.P.S., 2010, Difusão de massa em corpos cilíndricos: modelagem e desenvolvimento de software com aplicação à secagem de bananas, 129 p. Mestrado em Engenharia Agrícola, UFCG, PB, Brasil.

Silva, W.P., 2007, Transporte difusivo em sólidos com forma arbitrária usando coordenadas generalizadas, 263 p. Tese de Doutorado em Engenharia de Processos). Centro de Ciências e Tecnologia, UFCG, PB, Brasil.

Silva, W.P.; Silva, D.D.P. S.; Silva, C.D.P.S; Lima, A.G.B., 2007, Simulação numérica da transferência de massa em sólidos de revolução via volumes finitos e coordenadas generalizadas. 8º Congresso Iberoamericano de Engenharia Mecânica, Cusco, Peru.

Silva, W.P.; Silva, D.D.P.S.; Silva, C.M.D.P.S; Silva, C.D.P.S. 2008, Numerical simulation of the water diffusion in cylindrical solids. International Journal of Food Engineering, v. 4, n.2, iss.2, article 6.

Silva, W.P.; Precker, J.W.; Silva, D.D.P.S.; Silva, C.D.P.S; Lima, A.G.B., 2009, Numerical simulation of diffusive processes in solids of revolution via finite volume method and generalized coordinates. International Journal of Heat and Mass Transfer. doi: 10.1016/j.ijheatmasstransfer.2009.05.008.

Silva, W.P.; Silva, C.M.D.P.S; Farias, V.S.O.; Silva, D.D.P.S., 2010, Calculation of the convective heat transfer coefficient and cooling kinetics of an individual fig fruit**.** Heat Mass Transfer, v. 46, p. 371–380.

Ukrainczyk, N., 2009, Thermal diffusivity estimation using numerical inverse solution for 1D heat conduction. International Journal of Heat and Mass Transfer. v. 52, p. 5675-5681.

Wu, B.; Yang, W.; Jia, C., 2004, A three-dimensional numerical simulation of transient heat and mass transfer inside a single rice kernel during the drying process. Biosystems Engineering, v. 87, n. 2, p. 191-299.

6. RESPONSIBILITY NOTICE

The authors are the only responsible for the printed material included in this paper.